Accepted Manuscript

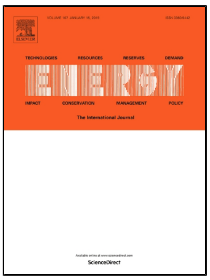

Analytical and Experimental Study of an Innovative Multiple-throughout-flowing Micro-channel-Panels-array for a Solar-powered Rural House Space Heating System

Yi Fan, Xudong Zhao, Guiqiang Li, Yuanda Chen, Jinzhi Zhou, Min Yu, Zhenyu Du, Jie Ji, Zishang Zhu, Thierno Diallo, Xiaoli Ma

PII:	S0360-5442(19)30050-7
DOI:	10.1016/j.energy.2019.01.049
Reference:	EGY 14522
To appear in:	*Energy*
Received Date:	16 September 2018
Accepted Date:	11 January 2019

Please cite this article as: Yi Fan, Xudong Zhao, Guiqiang Li, Yuanda Chen, Jinzhi Zhou, Min Yu, Zhenyu Du, Jie Ji, Zishang Zhu, Thierno Diallo, Xiaoli Ma, Analytical and Experimental Study of an Innovative Multiple-throughout-flowing Micro-channel-Panels-array for a Solar-powered Rural House Space Heating System, *Energy* (2019), doi: 10.1016/j.energy.2019.01.049

Analytical and Experimental Study of an Innovative Multiple-throughout-flowing Micro-channel-Panels-array for a Solar-powered Rural House Space Heating System

Yi Fan[a], Xudong Zhao[b,a,*], Guiqiang Li[a], Yuanda Chen[b], Jinzhi Zhou[a], Min Yu[a], Zhenyu Du[b], Jie Ji[c], Zishang Zhu[a], Thierno Diallo[a], Xiaoli Ma[a]

[a] School of Engineering and Computer Science, University of Hull, Hull HU6 7RX, UK

[b]College of Environmental Science and Engineering, Taiyuan University of Technology, China, 030024

[c]Department of Thermal Science and Energy Engineering, University of Science and Technology of China, 96 Jinzhai Road, Hefei City, 230026, China

*Corresponding author: Professor Xudong Zhao, xudong.zhao@hull.ac.uk

Abstract: This paper presents a combined analytical and experimental study of an innovative multiple-throughout-flowing micro-channel-panels-array applicable to a solar-powered rural house space heating system. This array, compared to the traditional one-to-one-connection panels-array, can significantly reduce the temperature difference between the head and real panels and thus increase the overall solar thermal efficiency and energy efficiency ratio (EER). The research methodology covers the theoretical analysis, experimental testing, model validation and system optimization. It is found that the analytical model has a good accuracy in predicting the performance of the multiple-throughout-flow micro-channels-panels-array, giving a discrepancy of less than 10%. In terms of the configuration and sizes of the array, 10 pieces of panels with 5 flow turns is regarded as the most favorite option. During the operation, decreasing flow rate of the fluid led to the increased EER of the panels-array. By converting the one-to-one-connection mode into the multiple-throughout-flowing mode, the overall solar thermal efficiency of the panels-array increases by around 10% and its energy efficiency factor (EER) decreases by 80% respectively. The research has addressed a novel solar-panels-array that can be well applied to solar thermal systems, thus making a significant contribution to the saving of fossil fuel

energy consumption and reduction of carbon emission on global scale.

Key words: Solar-thermal; Panels-array; Space heating; Multiple-throughout-flowing; Micro-channel; Thermal efficiency.

Nomenclature

A Area of the heat collection surface;

C_p Heat capacity of the working fluid;

D Internal diameter of the pipeline, 0.04m;

dT Temperature difference of working fluid between the inlet and outlet of the infinitesimal part of micro-channel, °C;

dy Length of the infinitesimal part of micro-channel, m;

F Fin efficiency;

F' Efficiency factor of micro-channel solar thermal panel;

F_R Thermal transfer factor of micro-channel solar thermal collector;

g Acceleration of gravity, m/s^2;

h Convective heat transfer coefficient, $W/m^2℃$;

h_f Frictional resistance, m;

h_m Local resistance, m;

I Solar radiation, W/m2;

L Width of the fin of the mini-channel, m;

l Length of the pipeline, 2m;

$\dot{m}$ Mass flow rate of working fluid, kg/s;

Nu Nusselt number;

n Number of the micro-channels in one tube;

Pr Prandtl Number;

Q_u Total quantity of heat, W;

q Quantity of heat by per square meter, W/m^2;

q' Quantity of heat by per unit length, W/m;

Re Reynolds number;

T	Temperatures, oC;
U	Heat loss coefficient, W/m2℃;
v	Velocity of the fluid, m/s;
y	Length of micro-channel, m;
α	Absorptivity of the glass layer;
η	Solar thermal efficiency;
ζ	Resistance coefficient of the local resistance;
τ	Transmittance of the glass layer;
λ	Heat conductivity coefficient of the working fluid, W/m℃;
λ_r	Resistance coefficient of the on-way resistance;
μ	Viscosity of the working fluid, Pa·s.

Subscripts

a	Ambient;
aq	Acquired solar radiation;
b	Bottom of solar thermal panel;
f	Working fluid;
fin	Fin of mini-channel;
$f.i$	Inlet of the working fluid;
$f.o$	Outlet of the working fluid;
fr	Frame of solar thermal panel;
L	Heat loss;
t	Top of solar thermal panel;
tube	Channel of the mini-channel;
u	Exploitative heat;
w	wall of the mini-channel;
$8-o$	Outlet of the eighth panel;
$1-i$	Inlet of the first panel.

1. Introduction

In 2012, annual energy consumptions of a household in China and EU were 1,426 kg and

2,000 kg[2] of standard coal respectively [1,2]; of which 45% was for space heating, 14% for hot water supply and 15% for electricity generation. Compared to the energy demand of residential buildings, the energies supplied by solar thermal and photovoltaic devices were very small, sharing only 2.6% of the overall energy demand in China and 1% in the EU. In line with this fact, the renewable solar energy technologies have huge potential of growth in building sector.

Traditional solar thermal collectors for space heating systems are classified as three categories: (1) flat plate collector, (2) glass vacuum tube collector, and (3) heat pipe collector [3] . Based on the EN12975-2 and ASHRAE 93 standards for solar collector testing, Rojas et al conducted an experimental testing to the selected flat-plate solar collector and the results showed that the incident angle modifier coefficient determined by the ASHRAE method was more accurate than that by the transient method according to the EN12975-2 standard, and the intercept solar efficiency of the flat-plate solar collector is around 62% [6]. Villar et al. developed a 3D model to simulate the performance of the flat-plate solar collector, indicating that the agreement between the model and the test is good and the intercept solar efficiency flat-plate is around 77% [7]. Budihardjo et al. carried out a numerical simulation of the the glass vacuum and flat-plate solar collectors, indicating that the performance of the glass vacuum tube solar collectors is high likely influenced by its low operational pressure and low fluid flow rate [8]. Liu et al carried out both the computer simulation and experimental testing of a high-performance evacuated tube solar water heater, indicating that ANN-based HTS method can effectively screen millions of designs with a proper algorithm, and predict the heat collection rates for each generated input [9]. Through a range of computer modeling and experimental tests, Speyer found that an evacuated heat pipe collector has a higher thermal efficiency than the flat-plate ones of the same sizes [10].

Currently, the micro-channel structure has been introduced into the construction of flat-plate solar collectors. owing to the smaller interior spaces compared to the traditional flat-plate panels, a micro-channel collector presents a superior performance on many aspects, i.e., higher heat transfer, lower convective heat loss, higher flow velocity and enhanced solar

efficiencies [11,12,13]. Deng studied the heat transfer performance of a micro-channel heat pipe array for the use in a flat plate solar collector (MHPA-FPC). The results showed that the MHPA-FPC has a higher heat transport capacity when increasing the cooling water flow rate and temperature [13]. Zhao et al investigated the performance of a novel flat plate solar collector with a micro-channel heat pipe array (MHPA-FPC), giving a solar thermal efficiency equation that has a slope of 5.6 and intercept factor of 0.85 [14,15]. Deng et al studied the performance of a photovoltaic/thermal system with a micro-channel-heat-pipe array that is used to provide hot water for the household, indicating that the system has an annual average daily effective heat gain of 9.5 MJ /m^2 and annual average system efficiency of 58.29% [16,17]. Li et al introduced a hybrid PV/thermoelectric module with a micro-channel heat pipe array that can increase its electrical output by making use of extra thermal energy reserved behind the PV module [18]. Mert Tosun et al integrated a mini-channel condenser into a household refrigerator [19]. Seunghyun Lee and Issam Mudawar studied the transient characteristics of flow boiling in large micro-channel heat exchangers [20].

It is apparent that a single solar panel cannot serve the space heating for a building. Instead, an array comprising numerous solar panels is applied. Zhao et al developed a solar heating system employing a one-to-one-connection PV/T solar thermal panels- array, giving the average electrical, thermal and overall efficiencies of 13.8%, 31.9% and 45.0% respectively [21]. Ling et al developed a solar thermal heating system using a type of connection combined with series and parallel connection, giving the thermal efficiency of 31.7% and the average indoor temperature of 14.9℃ [22]. Bava simulated the performance of the utilization factor of solar radiation for different row layouts, indicating that the connection method has significant impact on its solar efficiency [23]. Ion developed a novel solar-thermal collector with trapeze shape which is used as building block in arrays with various surface areas and well matching the variety of the building facades. As a result, three facades of single- and three of multi-family houses are comparatively analyzed considering architectural acceptance, functionality, durability (limited tracking) and thermal power output. [24]. Tian developed a validated TRNSYS-GenOpt model to optimize the key design

parameters of the connections of both collectors arrays, which indicates that parabolic trough collectors arrays are economically feasible for district heating networks in Denmark [25]. Within such an array, panels are always connected one after another. This connection manner creates a continuous temperature rise along the flow path. On the rear panels of the array, the fluid temperature reaches a very high level, which is especially the case for the a large-sized panels-array. As a result, the solar thermal efficiency of the rear panels will be significantly lower or even become a negative figure, owing to the inverse correlation between the panels' solar thermal efficiency and the temperature of the fluid across the panels. Therefore, the overall solar thermal efficiency of the array is smaller when the number of the panels in the array is larger. To tackle the challenges remaining with the one-to-one-connection panels-array, this research makes it first kind of effort to investigate a novel connection method with the multiple-throughout-flowing mode, which is a new connection approach among individual solar micro-channel panels that allows the working fluid to travel throughout the array for several times. Compared to the traditional one-to-one-connection mode, the new fluid flow mode based on the multiple-throughout-flowing can effectively lower the temperature of the panels at the rear of the array and reduce the temperature difference between the head and rear panels, thus leading to an increased overall solar thermal efficiency.

Based on the above identified innovation, this research conducted the analytical and experimental study of such a multiple-throughout-flowing micro-channel panels-array applicable to solar heating system. The results derived from the research would help wide adoption of the brand new solar panels-array and associated fluid flow pattern in various solar systems, thus making a significant contribution to the saving of fossil fuel energy consumption and reduction of the carbon emission on the global scale.

2. Concept development of the multiple-throughout-flowing micro-channel-panels-array and associated solar-driven rural house space heating system

Schematic of the proposed rural house solar-driven space heating system is shown in **Fig. 1**.

The system comprises a few innovative parts: (1) a multiple-throughout-flowing micro-channel panels-array which, owing to the reciprocating flowing of the fluid across the array, can effectively reduce the temperature difference between the head and rear panels of the array and thus increase the overall solar thermal efficiency compared to existing flat-plate solar collectors which are arranged in series (i.e., one-to-one-connection); (2) a dedicate sized PVs array which can achieve a balance between the sale profit of the PVs-generated electricity and purchase cost of the electricity used for the heat pump operation during winter season, thus achieving a zero-bill operation of the space heating system on the annual base; (3) a specialist heat exchanging/storage unit that allows the solar heat to be stored into the unit when the collected heat is greater than the heat demand of the building, and to be discharged into the loop water when the collected solar heat is less than the heat demand of the building. Furthermore, a dedicated electrical charge is also implemented into the unit that allows the charge of the grid electricity when solar energy is insufficient; and (4) alternative pipe routes (i.e., via or by-passing the heat exchanging/storage unit) that allow the fluid to be transported to the room under-floor heating coils directly when the loop fluid has a relatively lower temperature (e.g. <60℃), and to travel through the heat exchanging/storage unit when the loop fluid has a higher temperature (e.g. >60℃). The system is designed to provide space heating for a 150 m^2 rural house with the peak heat load of 10 kW. Technical specifications of the individual components of the system is presented in Table 1.

Table 1. The technical specifications of the components of the system

Name	Size	Technical index
PV panels	1m x 2m	Maximum output power: 300W
Solar thermal panels	1m x 2m	Maximum heat output: 1000W
Heat pump	1.5m x 0.5m x 1m	Nominal condition heating output: 12000W
Heat storage and exchange unit	Diameter: 1.19m, Height: 1.38m	Volume: 1.5m3
Under floor coil	Diameter: 16mm	Material: PE-X Length: 300m

This research mainly focuses on the characterization of the multiple-throughout flowing panels-array.

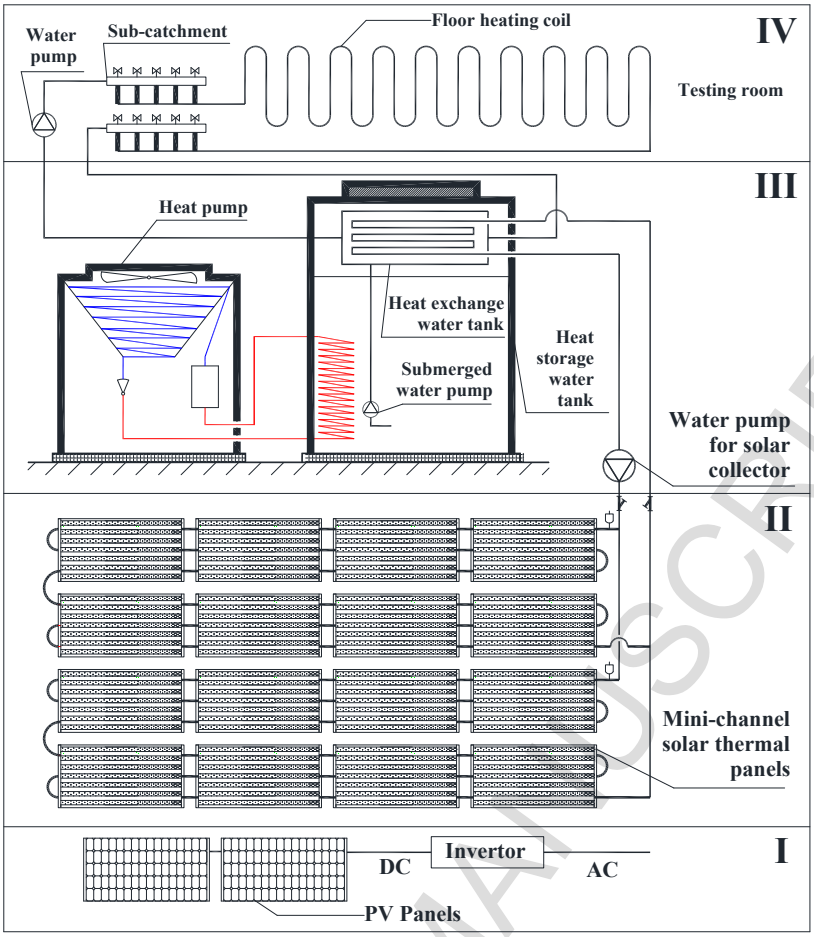

Fig. 1 The schematic of the micro-channel solar heating system employing the mini-channel solar thermal and PV panels

Based on this system platform, the multiple-throughout flowing micro-channle-panels-array will be studied, which is described in Section 3.

3. Analytical study of the multiple-throughout-flowing panels-array

3.1 Structure

Schematics of the both multiple-throughout-flowing micro-channel-panels-array and traditional one-to-one-connection micro-channel-panels-array are shown in **Figs. 2(a)** and **2(b)** respectively. Compared to the traditional one-to-one-connecting type, the new panels-array, by applying the multiple-throughout-flowing mode and associated connection method, can achieve a significantly higher solar thermal efficiency, owing to

the reduced temperature difference between the head and rear panels in the array, and increased flow rate of the fluid through the panels' cross section. Furthermore, this layout can also significantly reduce the flow resistance of the fluid across the panels in the array, owing to the reduced fluid turning number and reduced quantity of local fittings through its pathway (i.e., elbows, T-junctions, bends et al), thus leading to a significantly higher Energy Efficiency Ratio (EER) value. Based on the above system design platform, four panels of 1m x 2m each in an array are considered as the start point of the research.

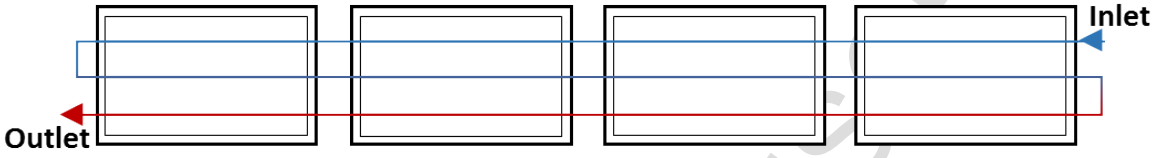

(a) Multiple-throughout-flowing type

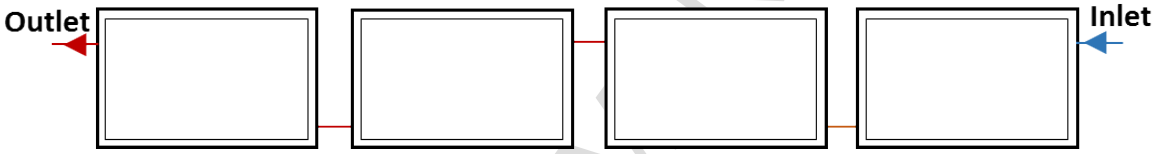

(b) Traditioal one-to-one-connecting type

Fig. 2 Schematics of the new and traditional solar panels arrays: (a) Multiple-throughout-flowing type; (b) Traditional one-to-one-connecting type

3.2 Efficiency-to-velocity correlation

The theoretical analysis below is based on a typical micro-channel flat-plate solar collector shown in **Figs. 3(a) and 3(b)**.

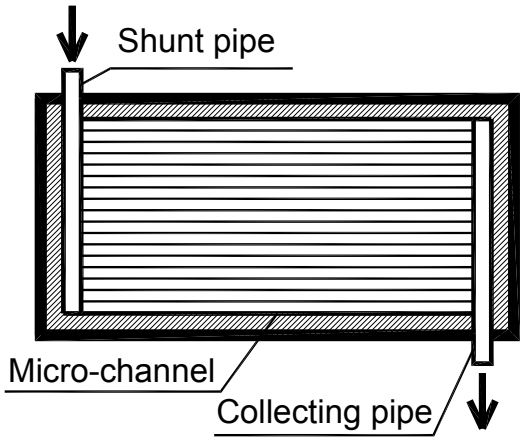

(a) Traditioal one-to-one-connecting type

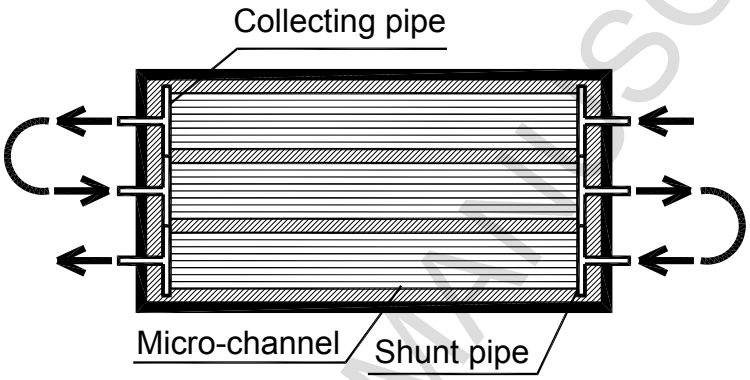

(b) Multiple-throughout-flowing type

Fig. 3 Two types of micro-channel flat-plate solar collectors

For the collector with one entry end and one exit end shown in **Fig. 3 (a)**, the standard test made by China National Center for Quality Supervision and Testing of Solar Heating System (Beijing) gave an experimental thermal efficiency equation, i.e., Eq. (1). Table 2 lists the measurement condition applied to this testing.

$$\eta = 0.73 - 3.5\frac{T_{f.i} - T_a}{I} \quad (1)$$

Table 2. Testing conditions at the national laboratory

Parameters	Testing circumstance
Mass flow rate	0.02kg/m^2·s
Solar radiation	600W/m^2
Wind speed	4m/s

The accuracy of the inlet temperature	±0.1℃
Accuracy of the ambient temperature	±0.5℃

As the area of the micro-channel solar thermal panel is 2m^2, the volume flow rate was set to 0.04kg/s which means the testing volume flow rate is 0.15m/h, and flow velocity in the micro-channel is **0.04m/s.** According to the parameters, the Reynolds number under the testing condition is 145.6. Taking this as the start point, this section will establish the correlation between the solar thermal efficiency and velocity.

When this type of solar collectors is applied to the arrays with one-to-one-connection mode shown in **Fig. 3(a)** and with multiple-throughout-flowing mode shown in **Fig. 3(b)**, the fluid flow velocity across the channel is 0.12m/s and 0.36 m/s respectively, which are higher than the velocity for the standard lab condition (0.04 m/s). To obtain the updated efficiency equations, the following analysis is conducted.

3.2.1 The efficiency factor of micro-channel solar thermal collector

The energy balance occurring in a solar thermal panel can be expressed as:

$$q_{aq} = q_u + q_L \tag{2}$$

In **Eq.2**, q_{aq} can be expressed as:

$$q_{aq} = I(\tau\alpha) \tag{3}$$

For the micro-channel solar panel, the solar energy reaching per meter length of the micro-channel strip **(shown in Fig. 4)** can be expressed as:

$$q'_{aq} = q_{aq}(2L + nD) \tag{4}$$

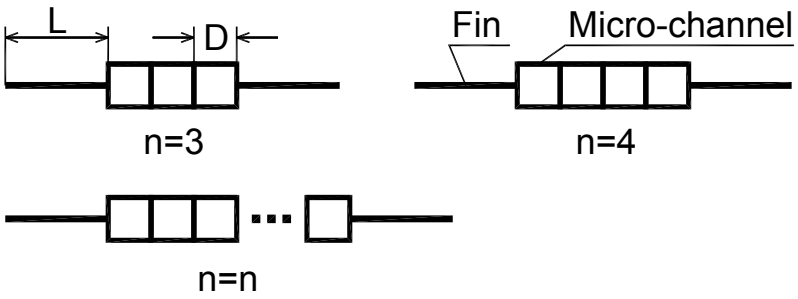

Fig. 4 Geometrical set-up of a single micro-channel tube

Furthermore, the heat absorbed by per meter length of a single micro-channel strip can also be expressed as:

$$q'_u = q'_{fin} + q'_{tube} \tag{5}$$

q'_{fin} and q'_{tube} can be further expressed as:

$$q'_{fin} = 2L[q_{aq} - U_L(T_w - T_a)] \tag{6}$$

$$q'_{tube} = nD[q_{aq} - U_L(T_w - T_a)] \tag{7}$$

In **Eqs. 6** and **7**, U_L can be expressed as:

$$U_L = U_t + U_b + U_{fr} \tag{8}$$

According to the configuration of the micro-channel solar thermal panel, the overall heat loss coefficient (U_L) can be considered to be 4.5 W/m^2·℃. The total heat absorbed by the panel q'_u is the sum of q'_{fin} and q'_{tube}, thus

$$q'_u = (2L + nD)[q_{aq} - U_L(T_w - T_a)] \tag{9}$$

The heat absorbed by per meter length of a single micro-channel strip can be expressed

as:

$$q_u^{'} = (2n+2)Dh(T_w - T_f) \tag{10}$$

In **Eq.10**, h can be expressed as:

$$h = Nu\frac{\lambda}{D} \tag{11}$$

$$Nu = 1.86Re^{1/3}\,Pr^{1/3}(D/l)^{1/3}(\mu_f/\mu_w)^{0.14} \tag{12}$$

Combining Eqs. 9 and 10 yields:

$$q_u^{'} = F^{'}[q_{aq} - U_L(T_f - T_a)] \tag{13}$$

$F^{'}$ is defined as the efficiency factor of micro-channel solar thermal collector which can be expressed as:

$$F^{'} = \frac{1/U_L}{\frac{1}{(2n+2)Dh} + \frac{1}{U_L(2LF+4D)}} \tag{14}$$

3.2.2 The thermal transfer factor of micro-channel solar thermal collector

The efficiency factor of a micro-channel solar thermal collector, $F^{'}$, used in **Eq.13** contains an unknown parameter, T_f. In this case, a known factor, $T_{f.i}$, should be used to calculate the absorbed heat $q_u^{'}$ instead of the unknown parameter T_f. This conversion process is described as below:

As shown in **Fig. 5**, an infinitesimal part of a micro-channel with a length of dy is used for this analysis; the heat carried by the entering flow and exiting flow can be represented by $\dot{m}C_pT_{f,y}$ and $\dot{m}C_pT_{f,y+dy}$ respectively.

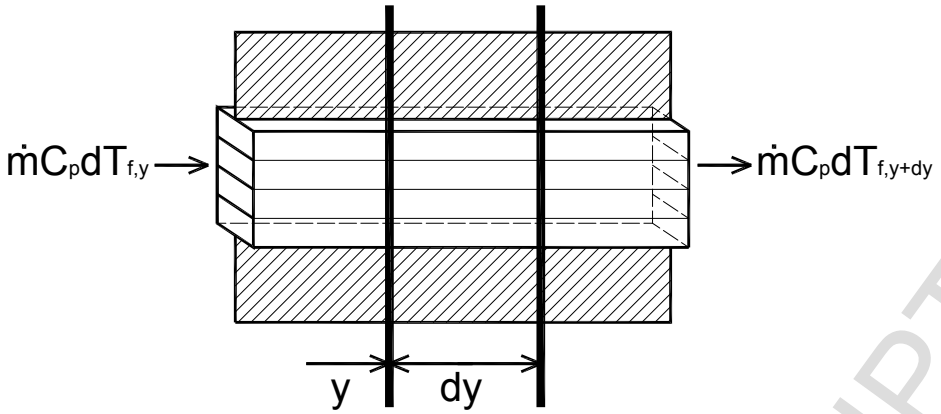

Fig. 5 Geometrical set-up of a micro-channel

The absorbed heat by this infinitesimal part of micro-channel with a length of dy can be expressed as:

$$\dot{m}C_p dT_f = q_u^{'} dy \qquad (15)$$

Combination of Eqs. 13, 15 and 16 yields,

$$\dot{m}C_p dT_f = F^{'}[q_{aq} - U_L(T_f - T_a)]dy \qquad (16)$$

Integrating the both sides of **Eq.16** yields,

$$\int \dot{m}C_p dT_f = \int F^{'}[q_{aq} - U_L(T_f - T_a)]dy \qquad (17)$$

Solving the integrating equation (17) yields:

$$\frac{T_f - T_a - q_{aq}/U_L}{T_{f.i} - T_a - q_{aq}/U_L} = \exp\,[-U_L F^{'} y/\dot{m}C_p] \qquad (18)$$

The length of micro-channel tube is l, which means the y in **Eq.18** equals l. As a result, the outlet temperature of working fluid ($T_{f.o}$) can be expressed as:

$$T_{f.o} = T_a + \frac{q_{aq}}{U_L} - \left[\frac{q_{aq}}{U_L} - (T_{f.i} - T_a)\right]\exp\,(-F^{'}U_L l/\dot{m}C_p) \qquad (19)$$

The absorbed heat by micro-channel can be expressed as:

$$Q_u = \dot{m}C_p(T_{f.o} - T_{f.i}) \quad (20)$$

The absorbed heat by per unit area micro-channel can be written as:

$$q_u = \frac{\dot{m}C_p}{(2L + nD)l}(T_{f.o} - T_{f.i}) \quad (21)$$

Bringing **Eq. 19** into **Eq. 21**, the absorbed heat by per unit length of micro-channel can be expressed as:

$$q_u = F_R[q_{aq} - U_L(T_{f.i} - T_a)] \quad (22)$$

F_R is the thermal transfer factor of the micro-channel solar thermal collector, which can be expressed as:

$$F_R = \frac{\dot{m}C_p}{(2L + nD)U_L}[1 - \exp(-F'U_L l/\dot{m}C_p)] \quad (23)$$

Based on the equations above, the heat transfer factors of the micro-channel solar thermal collector (F_R) relating to the three types of panels-arrays can be calculated and shown in **Table 3**.

Table 3. The heat transfer factors of the micro-channel solar thermal collector (F_R)

	Multiple-throughout -flowing	One-to-one connecting	One-to-one connecting (testing)
F_R	0.92	0.86	0.76

Solar thermal efficiency (η) of the panel can be expressed as:

$$\eta = \frac{q_u}{q_{aq}} \quad (24)$$

Combining Eqs. (22), (23) and (24) yields:

$$\eta = \frac{F_R[q_{aq} - U_L(T_{f.i} - T_a)]}{q_{aq}} = F_R(\tau\alpha) - F_R U_L \frac{(T_{f.i} - T_a)}{I} \quad (25)$$

For the one-to-one connection with u value of 0.04 m/s, the solar thermal efficiency

equation can be written as:

$$\eta = 0.74 - 3.3\left(\frac{T_{f.i} - T_a}{I}\right) \quad (26)$$

The theoretical equation (i.e., Eq.25) of solar thermal efficiency for one-to-one connecting methods under formal testing condition with u value of 0.04m/s has a good consistence with the equation (Eq.1) of the experimental efficiency equation which was developed by the China National Center for Quality Supervision and Testing of Solar Heating System (Beijing). This proves the availability and accuracy of the theoretical analysis.

For the one-to-one-connection type with u value of 0.12 m/s, $F_R = 0.86$, the thermal efficiency equation can be written as:

$$\eta = 0.81 - 3.6(\frac{T_{f.i} - T_a}{I}) \quad (27)$$

For the multiple-throughout-flowing type with u value of 0.36 m/s, F_R=0.92, thus, the thermal efficiency equation of the panel can be expressed as:

$$\eta = 0.92 - 4.1(\frac{T_{f.i} - T_a}{I}) \quad (28)$$

3.3 The overall solar thermal efficiency of the panels-arrays under the operational modes of 'multiple-throughout-flowing' and the 'one-to-one-connection'

3.3.1 'One-to-one-connection' mode

For the one-to-one connection mode, the thermal efficiency of a single panel is given as **Eq. 27**. Assuming the inlet temperature of the working fluid (water with glycol) of 25^{o}C, solar radiation of 600W/m^2, ambient temperature of 5^{o}C, and fluid flow rate of 0.5m^3/h which gives the channel velocity of 0.12m/s, and the temperature variation of the fluid throughout the 8 panels in the array can be obtained by using **Eq. 27**; this is shown in

Fig. 6.

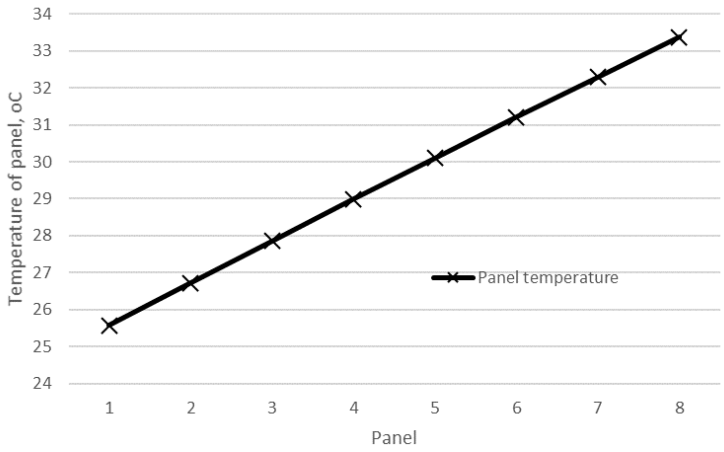

Fig. 6 Temperature variation of the fluid throughout the panels for the one-to-one connection mode

As a result, the overall efficiency of the whole panels-array is calculated by the following equation:

$$\eta = C_p \dot{m}(T_{8-o} - T_{1-i})/(8IA) \quad (29)$$

The thermal efficiency of different panels in the array is shown in **Fig. 7**; thus the overall solar thermal efficiency of the panels-array is 67%.

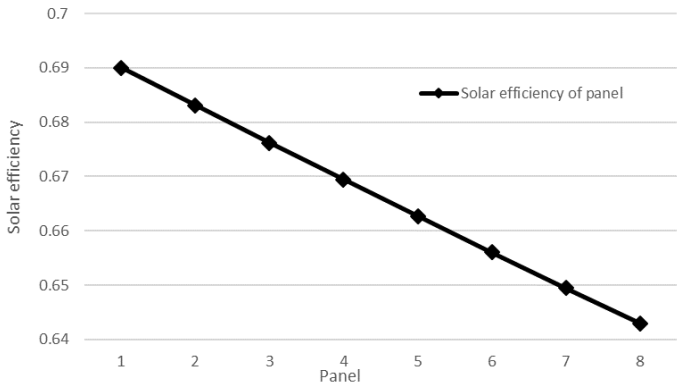

Fig. 7 Solar thermal efficiency variation throughout the panels for the one-to-one connection mode

3.3.2 'Multiple-throughout-flowing' mode

For the 'multiple-throughout-flowing' connection mode, the solar thermal efficiency of a single panel is given as **Eq. 28**. Assuming the same inlet temperature (i.e. 25°C) of the working fluid (i.e., water with glycol), solar radiation of 600W/m^2, ambient temperature of 5°C, and the same volume flow rate of 0.5m^3/h which gives the channel velocity of 0.36m/s, the temperature variation of the fluid at the different points of the panels can be obtained by using **Eq. 28**; these are showed in **Fig. 8**.

$$\eta = C_p m(t_{24} - t_0)/(8IA) \tag{30}$$

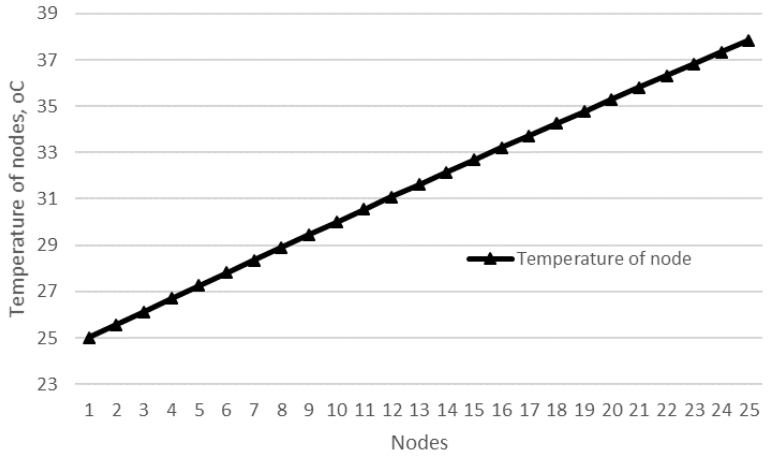

Fig. 8 Temperature along the nodes of panels for 'multiple-throughout-flowing' connection mode

The overall thermal efficiency of the panels-array is given by

$$\eta = Cpm(t_{24} - t_0)/(8IA) \tag{31}$$

For each individual panel, the solar thermal efficiency is given by

$$\eta 1 = (\frac{Cp\dot{m}(t_1 - t_0)}{\frac{IA}{3}} + \frac{Cp\dot{m}(t_{16} - t_{15})}{\frac{IA}{3}} + \frac{Cp\dot{m}(t_{17} - t_{16})}{\frac{IA}{3}})/3 \tag{32}$$

$$\eta 2 = \left(\frac{Cp\dot{m}(t_2 - t_1)}{\frac{IA}{3}} + \frac{Cp\dot{m}(t_{15} - t_{14})}{\frac{IA}{3}} + \frac{Cp\dot{m}(t_{18} - t_{17})}{\frac{IA}{3}}\right)/3 \quad (33)$$

$$\eta 3 = \left(\frac{Cp\dot{m}(t_3 - t_2)}{\frac{IA}{3}} + \frac{Cp\dot{m}(t_{14} - t_{13})}{\frac{IA}{3}} + \frac{Cp\dot{m}(t_{19} - t_{18})}{\frac{IA}{3}}\right)/3 \quad (34)$$

$$\eta 4 = \left(\frac{Cp\dot{m}(t_4 - t_3)}{\frac{IA}{3}} + \frac{Cp\dot{m}(t_{13} - t_{12})}{\frac{IA}{3}} + \frac{Cp\dot{m}(t_{20} - t_{19})}{\frac{IA}{3}}\right)/3 \quad (35)$$

$$\eta 5 = \left(\frac{Cp\dot{m}(t_5 - t_4)}{\frac{IA}{3}} + \frac{Cp\dot{m}(t_{12} - t_{11})}{\frac{IA}{3}} + \frac{Cp\dot{m}(t_{21} - t_{20})}{\frac{IA}{3}}\right)/3 \quad (36)$$

$$\eta 6 = \left(\frac{Cp\dot{m}(t_6 - t_5)}{\frac{IA}{3}} + \frac{Cp\dot{m}(t_{11} - t_{10})}{\frac{IA}{3}} + \frac{Cp\dot{m}(t_{22} - t_{21})}{\frac{IA}{3}}\right)/3 \quad (37)$$

$$\eta 7 = \left(\frac{Cp\dot{m}(t_7 - t_6)}{\frac{IA}{3}} + \frac{Cp\dot{m}(t_{10} - t_9)}{\frac{IA}{3}} + \frac{Cp\dot{m}(t_{23} - t_{22})}{\frac{IA}{3}}\right)/3 \quad (38)$$

$$\eta 8 = \left(\frac{Cp\dot{m}(t_8 - t_7)}{\frac{IA}{3}} + \frac{Cp\dot{m}(t_9 - t_8)}{\frac{IA}{3}} + \frac{Cp\dot{m}(t_{24} - t_{23})}{\frac{IA}{3}}\right)/3 \quad (39)$$

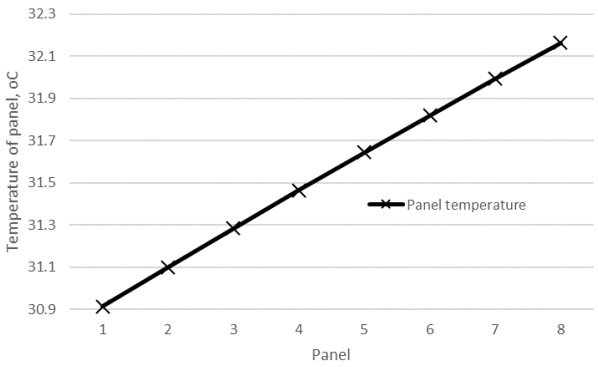

Fig. 9 Temperature variation of the fluid throughout the panels in the multiple-throughout-flowing connection mode

The temperature variation of the fluid throughout the panels in the array is shown in Fig. 9. Furthermore, Fig. 10 indicates the average thermal efficiency of the different panels in an array, thus, the overall thermal efficiency of the panels-array is 74%.

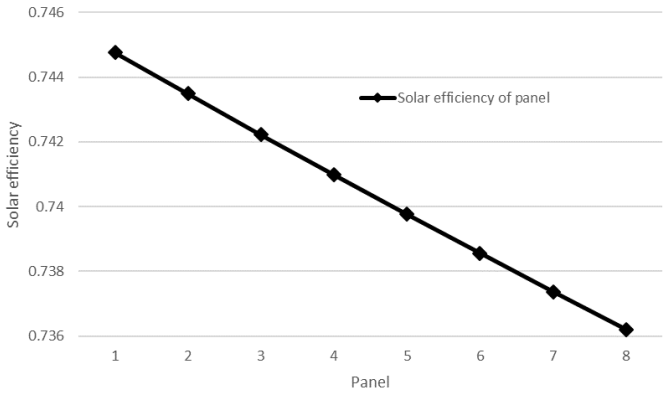

Fig. 10 Solar efficiency variation throughout the panels in the 'multiple-throughout-flowing' connection mode

3.3.3 Comparison between the 'one-to-one-connection' and 'multiple-throughout-flowing' modes

Figs. 11 and **12** show the comparison between multiple-throughout-flowing and one-to-one-connecting modes, which give the panels' average temperature and associated solar thermal efficiency respectively. For an array with 8 panels, the multiple-throughout-flowing mode can achieve 10.4% higher solar thermal efficiency compared to the one-to-one-connection mode (74% against 67%). The temperature of the panels at the rear of the array will be reduced from 33.4°C to 32.2°C, leading to the increase of its thermal efficiency by 14.5% (i.e., from 64.3% to 73.6%). Furthermore, the temperature difference between the head and rear panels of the array will be reduced by 84%, leading to the increased overall solar thermal efficiency by 10.4% (i.e., from 67% to 74%).

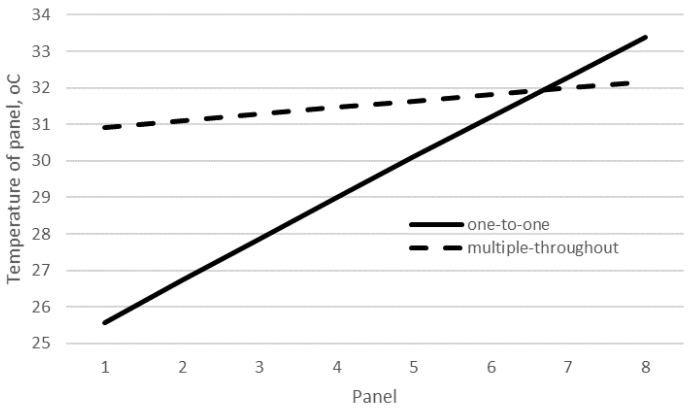

Fig. 11 Temperature variation of the fluid through the panels

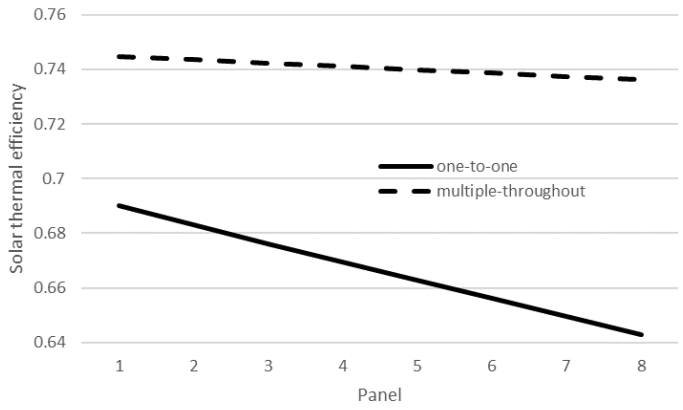

Fig. 12 Solar thermal efficiency variation through the panels

The comparison of the fittings and local resistance factor between two configurations can show another advantage of the multiple-throughout-flowing configuration. The flow resistance of the fluid across the panels-array can be calculated in the following way:

The resistance through the pipeline can be divided into two parts: the local resistance and the along-the-way frictional resistance. The equations of the along-the-way frictional resistance can be given as:

$$h_f = \lambda_r \frac{l}{D} \frac{v^2}{2g} \tag{40}$$

$$h_m = \zeta \frac{v^2}{2g} \tag{41}$$

According to the above formulas, the pipe resistance at every node along the pipeline can be theoretically calculated, and the results are shown in **Fig.13**. The pipe resistance of both connection configurations shows an approximate linear increasing trend along the pipeline. However, owing to the larger number of elbows in the one-to-one configuration compared to the multiple-throughout-flowing, the pipe resistance of the one-to-one configuration grew much faster than that of the multiple-throughout-flowing. As a result, with the same number of the solar thermal panels, i.e., 8 panels, and under same flow volume rate, i.e., 0.5m^3/h, the total pipe resistance of the one-to-one connection configuration is around 6 m higher than that of the multiple-throughout-flowing mode. Furthermore, the results based on the theoretical

calculation is very close to the data collected from the on-site testing, indicating that the theoretical calculation can be used to determine the pipe resistance.

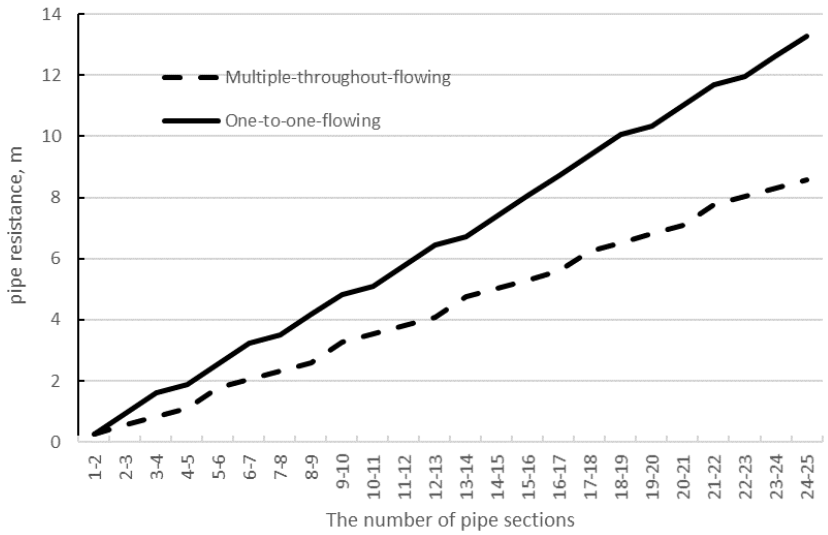

Fig. 13 Pipe resistance along the flowing path

The flow resistance of the fluid across the multiple-throughout-flowing array is significantly lower than that in the one-to-one flowing array (8m vs. 13m). Meanwhile, the heat output from the multiple-throughout-flowing array is 10.4% higher than that from the one-to-one-flowing array. This leads to a significantly higher Energy Efficiency Ratio (EER) (i.e., a ratio of the collected heat to the consumed energy by the solar thermal collector, shown in Eq.42) in the multiple-throughout-flowing array compared to the one-to-one-connection array.

$$EER = \frac{Q_{aq}}{W_c} \tag{42}$$

The EERs for the one-to-one-connection and multiple-throughout-flowing modes are 205 and 368 respectively, indicating that the multiple-throughout-flowing mode has a 79.5% higher EER compared to the one-to-one type; this represents another advantage of the multiple-throughout-flowing mode.

4. Experimental set up and results analysis, as well as validation/refinement of the analytical model

4.1 Experimental set-up

An experimental system was established to test the performance of different panels-arrays. This system, as shown schematically in **Fig. 1**, comprises a set of panels-array which could be either multiple-throughout-flowing type or one-to-one-connection type. Detailed information of it is presented as below:

Multiple-throughout-flowing panels array

Four individual panels are arranged in the form of multiple-throughout-flow connection, while other four individual panels are similarly arranged. The two arrays are then connected in series and the whole image of the panel connection is shown in **Fig. 2(a)**.

Such an individual panel, as shown in **Figs. 14** and **15**, comprises a few functional layers: (1) the professional glazed cover for solar thermal panel to prevent the heat loss and protect the thermal panels; (2) the air layer to provide a gap between the panel and glaze thus reducing the heat loss to surrounding; (3) the black chrome absorber layer to increase the absorptivity of the panel to solar irradiance; (4) the mini-channels layer (28 mm x 5 mm), which has numerous mini-channel rectangular pipes and is connected to the head tubes on both ends; (5) the insulation layer to minimize the heat loss of the panel to the surrounding; and (6) holding-up framework. The photograph of the panel is presented in **Fig. 16**, while the sizes and material of each component are shown in **Table 3**.

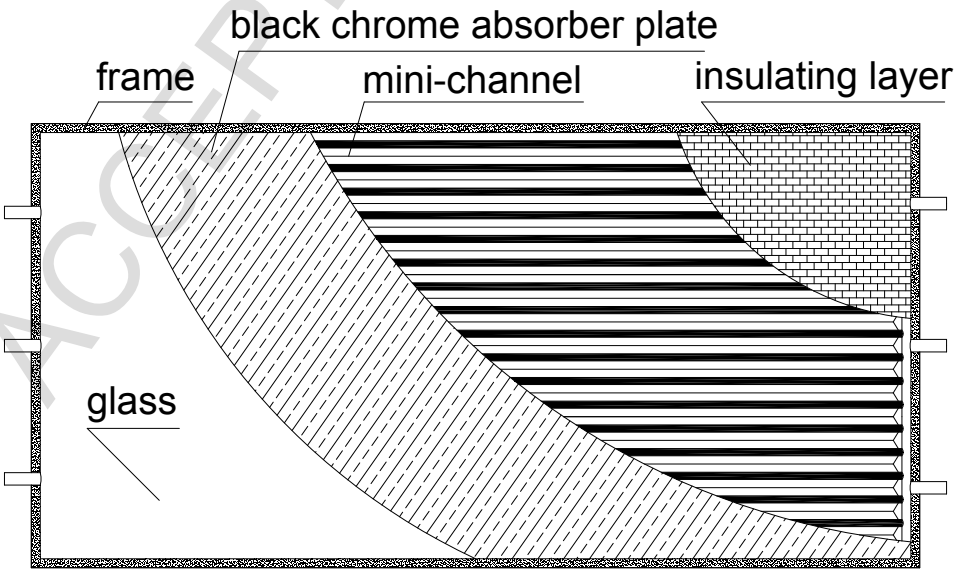

Fig. 14 Front view of the mini-channel solar thermal panel

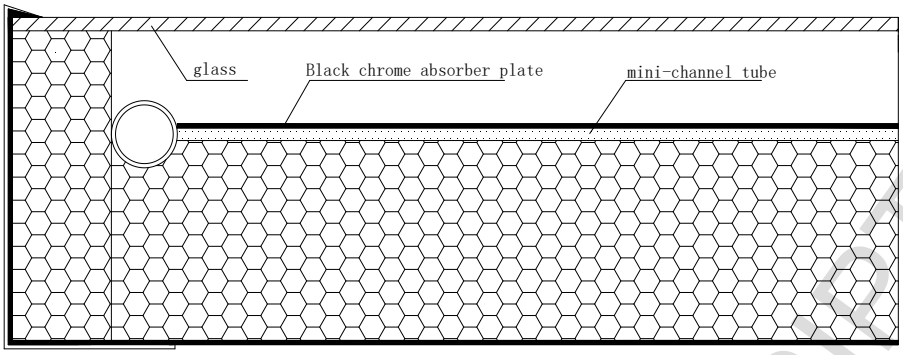

Fig. 15 A sectional view of the mini-channel solar thermal panel

Fig. 16 The photograph of the mini-channel solar thermal panel

Table 4. Sizes and materials of the mini-channel solar thermal panel

No	Element	Thickness	Function
1	Low iron tempered glass plate	3.2mm	Based panel; prevent dust and rain water
2	Black chrome absorber plate	0.1mm	Enhance solar thermal efficiency
3	Mini-channel tube	4mm	The flow channel of Refrigerant
4	Phenolic plate	62mm	Thermal insulation layer
5	Frame	80mm	Packaging, fix, protection

One-to-one-connection panels-array

Alternatively, eight individual panels are arranged in one-to-one-connection manner; the whole image of the panels-array is shown in **Fig. 2(b)**. The technical specifications of the individual panels are referred to **Table 4**, which is same as the data for the panels in multiple-throughout-flowing connection.

Heat exchange and storage tank

There are four main functional parts in the heat exchange and storage tank, including: (1) a heat exchange water tank at the top of the outer heat storage water tank; (2) a heat storage tank containing 1.5m^3 of water and a submerged water pump, which is dedicated to store heat to the tank water when the solar irradiation is high and release heat to the room space when the solar irradiation is low; (3) a set of coil-type-heat-exchanger embedded into the bottom of the heat storage water tank, connecting to a heat pump to supply auxiliary heat for the system; and (4) a hot water supply part merged into the bottom of the heat storage water tank with a set of coil-type-heat-exchanger; two sides of which are connected to the water supply network and the domestic water supply pipe separately. The photograph of the heat storage tank is shown in **Fig. 17**, while its technical data are listed in **Table 5**.

Fig. 17 Photograph of the heating tank

Table 5 The technical data of the heat exchange and storage water tank

Storage tank value			
Height	1380 mm	Area	0.66 m^2
Diameter	1190 mm	Volume	1.5 m^3
Thickness of insulation	50 mm		

4.2 Testing instrument and procedure

Based on the above design and components selection, two identical experimental systems, one with a multiple-throughout-flowing panels-array and other with a one-to-one-connection panels-array, were established. These systems were installed with various measurement instruments and sensors. Within the systems, the temperature, flow rate and pressure of the

fluid in the solar loop and room heating loop were measured using the platinum resistance thermometer probes, flow meters and pressure gauges, respectively, which were appropriately implemented into the systems. All the outputs of the sensors and instruments in a system were transmitted into a Data Logger and then to a computer. The specifications, quantity, and installation position of the sensors/meters used in the measurement process are outlined in **Table 6**. The tests were carried out under the real-time operational condition in a typical rural house in Lvliang city China, throughout consecutive 10 days, i.e., 21st and 30th December 2017. Lvliang city has a typical dry climatic condition and enjoys the sun shining on most days of a year. All the testing results were obtained under the practical weather condition in the selected 10 days.

Table 6 List of experimental testing and monitoring devices

Devices	Specifications	Quantity	Location
Pyranometer	TQB-2C (Sunlight, China)	1	Top of the collector
Water flowmeter	LWGY-MK-DN25(MACON China)	2	One branch of solar thermal panels; solar thermal panels main entrance;
Anemometer	HS-FS01(Huakong single, China)	1	Top of the collector
Platinum resistance thermometer	PT1000(Zhongjia China)	40	solar thermal panels; testing room; water tank; ambient, etc.
Data logger and computing unit	34970A (Agilent, USA)	1	Testing room
Pressure gauge	YN60 0-0.6Mpa (Jiangyin, China)	6	Inlet and outlet of water pump; Inlet and outlet of solar thermal panels; Inlet and outlet of the water tank;

4.3 Results analysis and comparison between the modeling and experimental data

4.3.1 Solar efficiency against $(T_{in} - T_a)/I$

Based on the experimental data of the two parallel systems, a variation of the solar efficiencies of the panels-arrays against $(T_{in} - T_a)/I$ were established and these are depicted in **Figs. 18** and **19** respectively. Meanwhile, the above established model will be run on the basis of variation of $(T_{in} - T_a)/I$, which will be made by keeping the Tin and Ta unchanged (i.e., 25oC and 5oC) and varying solar radiation from 100 W/m2 to 600 W/m2. Pulling together both the modeling and experimental data in the same

Figures (**Fig. 18** for the multiple-throughout-flowing mode and **Fig. 19** for the one-to-one-connection mode) indicates that both experimental results and modeling data have good agreement each other, with derivation ratio in the range 0.1% to 10%.

Comparison between **Figs. 18** and **19** indicates that under the same value of $(T_{in} - T_a)/I$, the overall solar thermal efficiency of the multiple-throughout-flowing panels-array is higher than that of the one-to-one-connection panels-array, with the increase rate in the range 0.5% to 10%. This further approves the advantage of the multiple-throughout-flowing type panels-array.

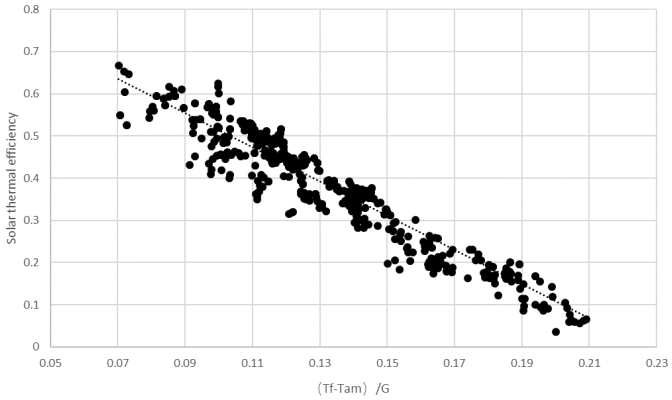

Fig. 18 Solar efficiency against $(T_{in} - T_a)/I$ for the multiple-throughout-connecting type

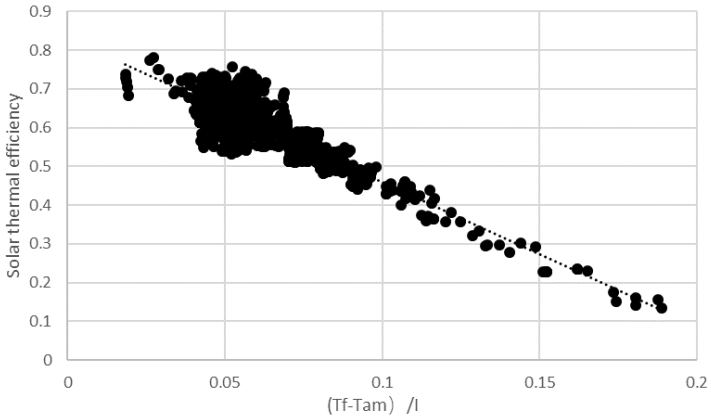

Fig. 19 Solar efficiency against $(T_{in} - T_a)/I$ for the one-to-one-connection flowing type

4.3.2 EER against $(T_{in} - T_a)/I$

Based on the experimental data of the two parallel systems, variation of the Energy Efficiency Ratios of the panels-arrays against $(T_{in} - T_a)/I$ can also be established and these are depicted in **Figs. 20** and **21** respectively. Meanwhile, the above established model will run on the basis of the variation of $(T_{in} - T_a)/I$, which will be made by keeping the T_{in} and T_a unchanged (i.e., 25°C and 5°C) and varying solar radiation from 100 W/m^2 to 600 W/m^2. Pulling together both the modeling and experimental data in the same figures (**Fig. 20** referring to the multiple-throughout-flowing mode and **Fig. 21** to the one-to-one-connection mode) indicates that both experimental results and modeling data have good agreement each other, with derivation ratio in the range 0.1% to 10%.

Comparison between **Figs. 20** and **21** indicate that under the same value of $(T_{in} - T_a)/I$, the overall Energy Efficiency Ratio of the multiple-throughout-flowing panels-array is significantly higher than that of the one-to-one-connection panels-array, with the increase rate in the range 62% to 68%. This indicates that the multiple-throughout-flowing type is superior to the traditional one-to-one-connection type.

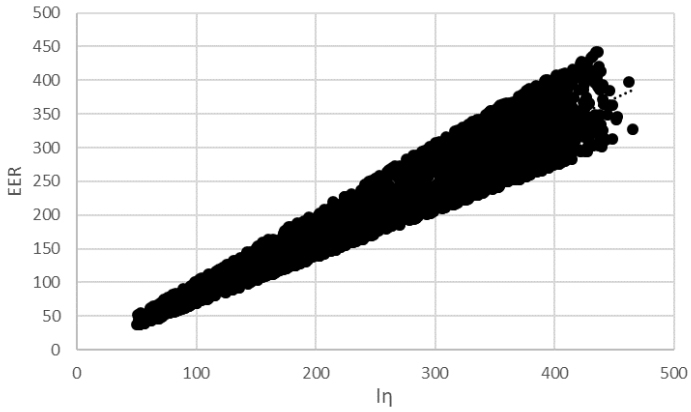

Fig. 20 EER against $I\eta$ for multiple-throughout-connecting type

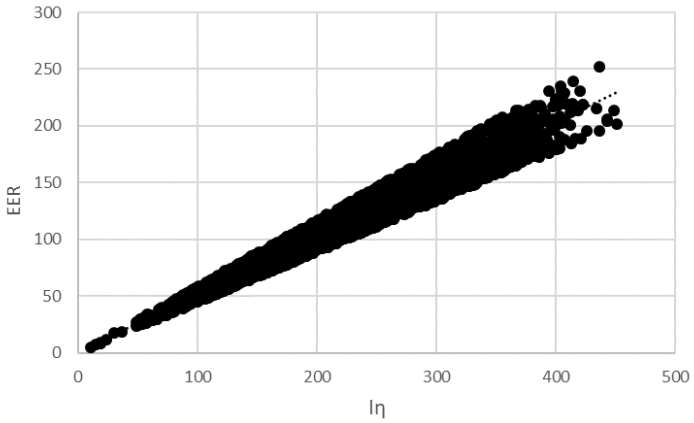

Fig. 21 EER against $I\eta$ for one-to-one connecting type

4.3.3 Temperature variation across the panels-arrays

To facilitate the comparison between the modeling and experimental results, the measurement data for a selected single winter day (i.e., 24th December 2017) were extracted. These data, including those for the fluid's inlet temperature, ambient temperature, air velocity, fluid flow rate, were further divided into three groups according to the relevant time zones, i.e., 9:00 to 12:00, 12:00 to 15:00, and 15:00 to 18:00. For each time zone, the data for each single parameter were averaged, thus giving the average value of this parameter which forms the foundation of the consequent parallel simulation.

The average data of the temperature of the working fluid of each panel as three different time zones are depicted in **Figs. 22** and **23** respectively which refer to the multiple-throughout-flowing and one-to-one-connection modes. Meanwhile, the above-established model was run based on the average data for an inlet temperature and flow rate of the fluid, as well as ambient temperature. This gave the average data of the fluid temperature at the outlet of each panel. Pulling together the modeling and experimental data together in the same Figures (**Fig. 22** referring to the multiple-throughout-flowing mode and **Fig. 23** to the one-to-one-connection mode) gives a good comparable image for both the experimental results and modeling data; this indicates that a good agreement was achieved between the both, with derivation ratio in the range **0.3% to 8.1%.**

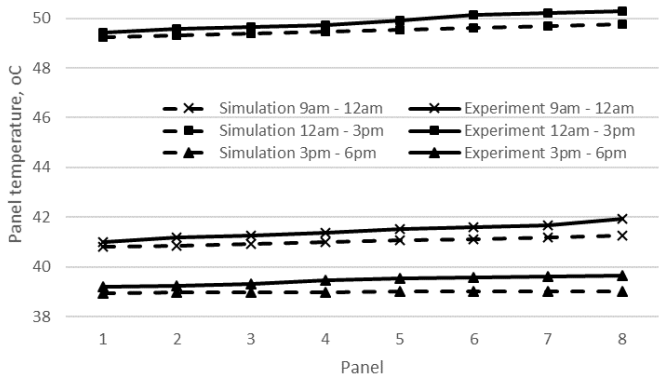

Fig. 22 The average temperature of the working fluid of each panel at three different time zones for the multiple-throughout-flowing type

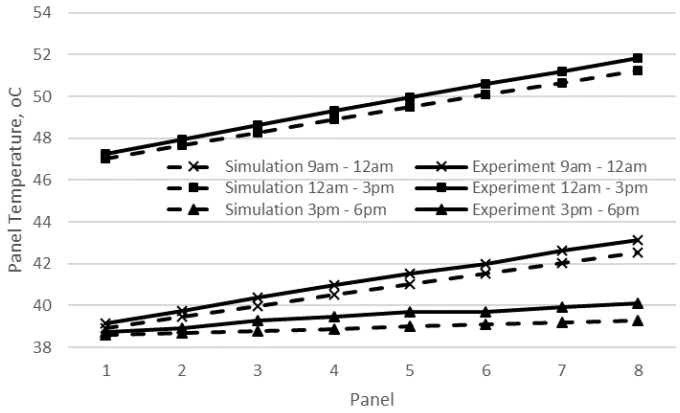

Fig. 23 The average temperature of the working fluid of each panel at three different time zones for the one-to-one connecting type

Comparison between **Figs. 22** and **23** indicates that under the same operational condition (i.e., same flow rate and inlet temperature and ambient temperature), the temperature of the working fluid at the outlet of the rear panel is lower for the multiple-throughout-flowing panels-array compared to the one-to-one-connection type, with a difference in the range **0.6% to 3%.** The temperature difference between the head and rear panels in the multiple-throughout-flowing model is lower than that in the one-to-one-connection mode. This indicates the multiple-throughout-flowing type can effectively reduce the temperature of the rear panel in an array compared to the

one-to-one-connection array. It can also effectively lower the temperature difference between the head and read panels in an array, thus improving the overall thermal efficiency of the array.

4.3.4 The solar thermal efficiency of the different panels for two types of arrays

Similarly, the experimental solar thermal efficiency of the individual panels under three different time zones was depicted into **Figs. 24** and **25** respectively, which are for the multiple-throughout-flowing and one-to-one-connection modes respectively. Meanwhile, the above-established model was run based on the average data for the inlet temperature and flow rate of the fluid, as well as ambient temperature. This gave the solar thermal efficiency data of the panels in two different arrays. Pulling together both the modeling and experimental data in the same figures gives a good comparable image of both the experimental results and modeling data, indicating that a good agreement was achieved between the both, with derivation ratio in the range **1% to 9%**.

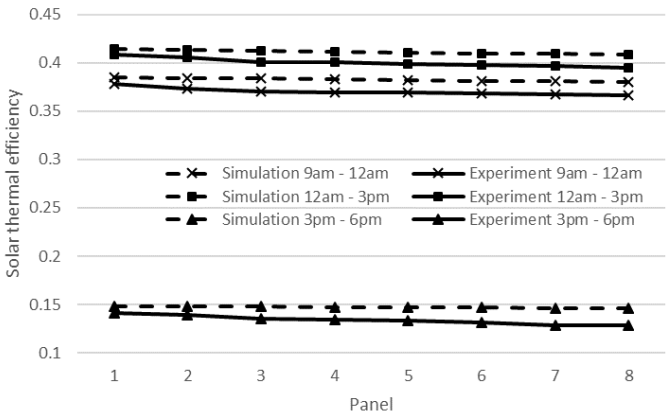

Fig. 24 The solar thermal efficiency of the individual panels under three different time zones for the multiple-throughout-flowing type

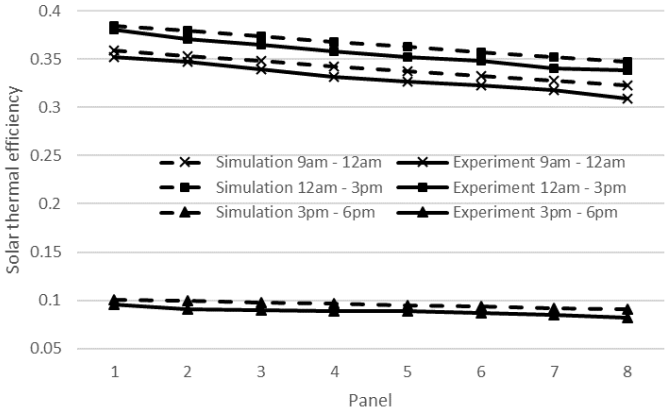

Fig. 25 The solar thermal efficiency of the individual panels under three different time zones for the one-to-one connecting type

Comparison between **Figs. 24** and **25** indicates that for the multiple-throughout-flowing mode, the solar thermal efficiency of the head panel is somehow lower than that of the one-to-one-connection mode. However, the solar thermal efficiency of the rear panel is higher than that of the one-to-one-connection mode. As a result, the overall solar thermal efficiency of the multiple-throughout-flowing array is higher than that of the one-to-one-connection array, with the increasing ratio of around 5%. This indicates that the multiple-throughout-flowing mode is an effective measure of increasing solar thermal efficiency of the panels-array, compared to the one-to-one-connection mode.

5 Further optimal study and results discussion

Based on the above validated computerized model and experimental conditions, further simulation and optimization were carried out to determine the best geometrical set-up and operational condition. This involves the determination of the best panel number, piping turning number, as well as the appropriate velocity of the fluid flow.

5.1 Impact of the number of panels in an array

Impact of the panels' number to the performance of the system was investigated by fixing other parameters in 6 situations (shown in **Table 7**) and varying the number of the panels from 5 to 25.

Table 7 Operational conditions

No.	Inlet Temperature (°C)	Ambient temperature (°C)	Solar Radiation (W/m^2)	(Tin – Ta)/I
1	23	5	600	0.03
2	47	5	600	0.07
3	65	5	600	0.1
4	25	5	666.6	0.03
5	25	5	285.7	0.07
6	25	5	200	0.1

As shown in Table 6, the solar radiation and ambient temperature are same for situation No.1 to No.3, the solar radiation is the variant in these three situations. And the inlet temperature and ambient temperature are same for situation No.4 to No.6, the solar radiation is the variant in these three situations. As a result, the analyzing will take situation No.1 to No.3 as a group and No.4 to No.6 as a group respectively.

The overall solar thermal efficiency of the panels-array against the panel number under the situation No.1 to No.3 and No.4 to No.6 is shown in **Fig.26** and **Fig.27**. It is found that the solar thermal efficiency of the panels-array decreases with the number of panels increasing from 5 to 25, indicating that the solar efficiency of panels-array is in inverse proportion to the number of panels. The reason for this phenomenon lies in the increased temperature of the panels at rear part of the array which leads to the reduced overall solar thermal efficiency with the increased panels' number.

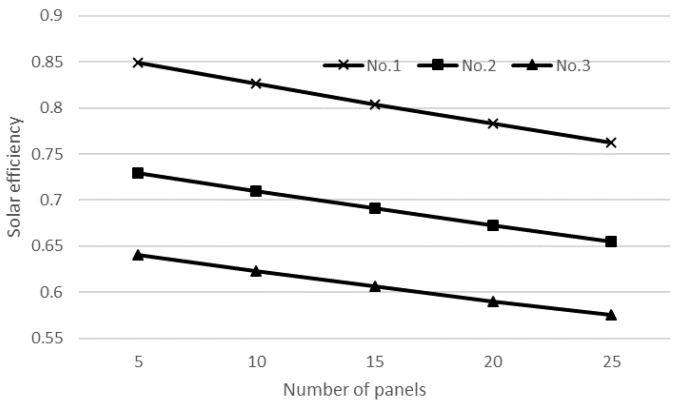

Fig. 26 The variation of the solar thermal efficiency under situation No.1 to No.3

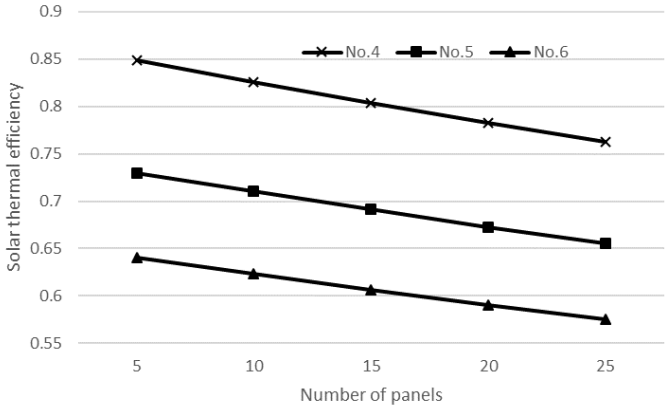

Fig. 27. The variation of the solar thermal efficiency under situation No.4 to No.6

Meanwhile, the EER against the panels' number under the situation No.1 to No.3 and No.4 to No.6 is shown in **Fig.28** and **Fig.29.** It is found that the EER of panels-array initially increases with the increase of the panels' number and then decreases with the increase of the panels' number, and the maximum EER of the panels-array occurs at the panel number of 10. This can be explained as such: when increasing number of the panels in an array, the heat output of the array is in fast growth trend and meanwhile, the power consumption of the pump also grows steadily. The ratio of the heat output to the pump power is quickly going up and when the panels' number is above 10, this ratio value falls owing the fast-growing fluid flow resistance and less fast increase in the array's heat output.

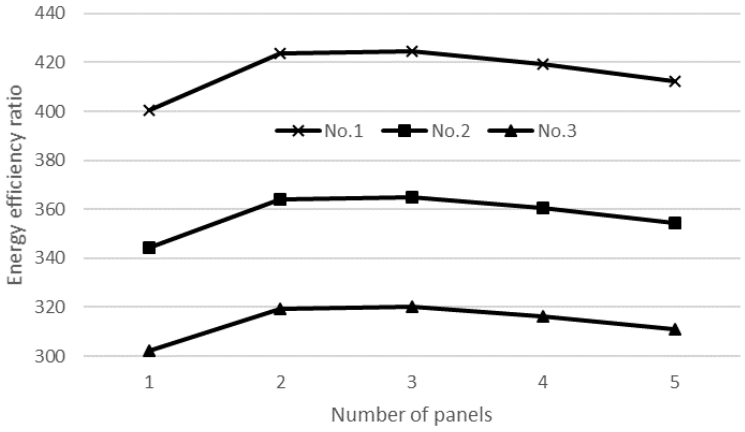

Fig. 28 The variation of the energy efficiency ratio under situation No.1 to No.3

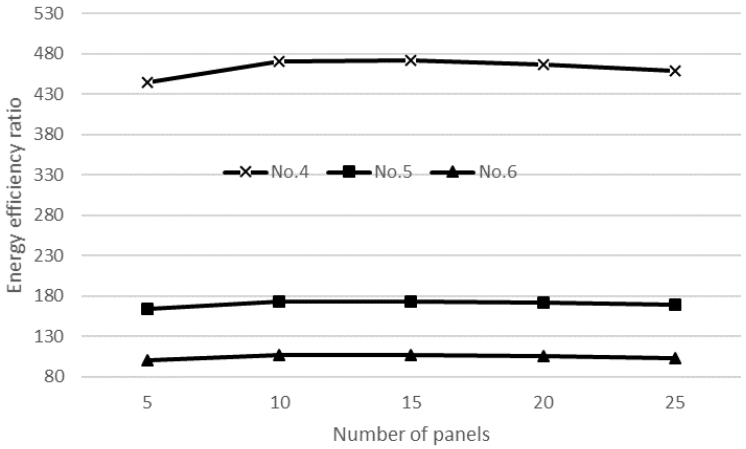

Fig. 29 The variation of the energy efficiency ratio under situation No.4 to No.6

5.2 Impact of the turning number of panels in an array

According to the results, under different circumstances, the variations of the solar thermal efficiency and the solar EER are similar. Hence, for analyzing the other characteristics of the solar thermal collectors' array, No.1 situation is used for analyzing, which is shown in **Table 6.**

Impact of the fluid flow turning number was investigated by fixing other parameters (shown in **Table 6**) and varying the turning number from 2 to 10. The overall efficiency of the panels array against the fluid flow turning number is shown in **Fig 30**. It is found that increasing the fluid flow turning number within an array leads to the continuous growth of the solar thermal efficiency of the array. However, the growth rate is higher when the turning number is less than 5 and this is getting lower when the turning number is more than 5.

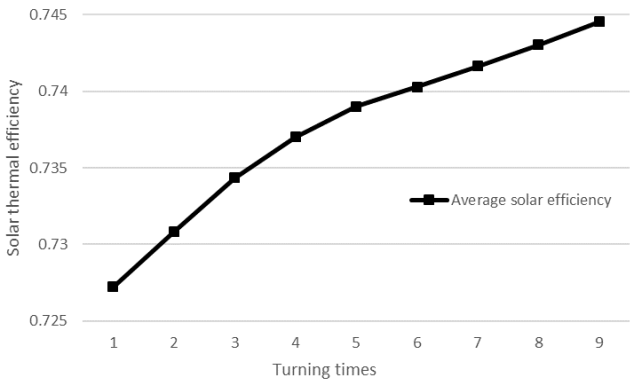

Fig. 30 Solar thermal efficiency with different fluid flow turning number for the multiple-throughout-flowing type

Fig.31 shows the variation of the EER of the array against the fluid flow turning number. It is found that increasing the fluid flow turning number within an array leads to the continuous fall of the solar thermal efficiency of the array. However, the reduction rate of the EER is initially higher when the turning number is less than 5 and this is getting lower when the turning number is more than 5.

Combination of the both Figs. Indicates that the adequate fluid flow turning number is 5; beyond which the performance of the panels' array tends to more stable with less dramatic change in both the solar thermal efficiency and EER.

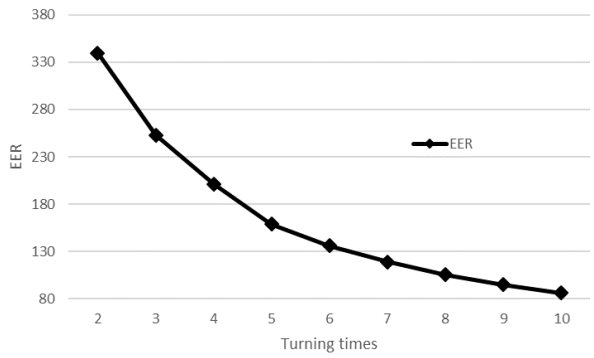

Fig. 31 EER with different fluid flow turning number for the multiple-throughout-flowing type

5.3 Impact of the fluid flow speed in an array

Impact of the fluid flow speed was investigated by fixing other parameters (shown in **Table 6**) and varying the volume flow rate from 0.1m^3/h to 1m^3/h. The overall efficiency of the panels array against the panel number is shown in **Fig 32**. It is found that increasing the fluid flow speed leads to continuous increase in volume flow rate and fluid flow speed, indicating that a higher fluid speed benefits to the performance of the panels-array. However, the solar thermal efficiency experiences a very fast growth when the volume flow rate increases from 0.1m^3/h to 0.3m^3/h; the growth rate tends to be slow when the flow rate exceeds 0.3m^3/h.

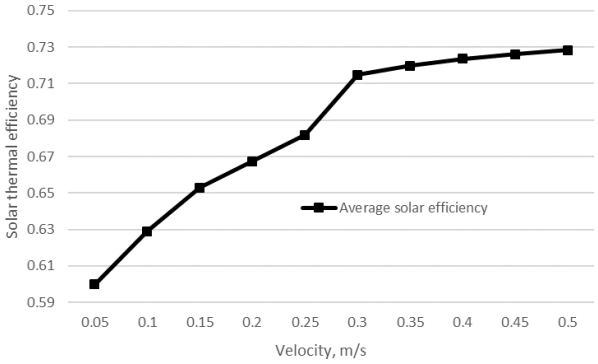

Fig. 32 Solar thermal efficiency with different volume flow rate for the multiple-throughout-flowing type

Variation of the EER against the fluid flow rate (speed) is shown in **Fig. 33**. It is found that increasing the fluid flow speed leads to continuous fall in energy efficiency rate (EER), indicating that a higher fluid speed has a negative effect to energy performance of the panels array. The fast fall of the EER occurs when the fluid flow velocity varies from 0.1m/s to 0.3m/s; this figure tends to be less varying when the flow rate exceeds 0.3m/s. This again proves that the most favorite flow speed is 0.3m/s from solar collection effect.

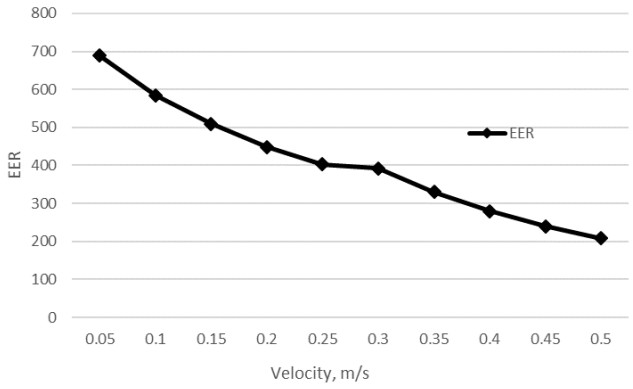

Fig. 33 EER with different volume flow rate for the multiple-throughout-flowing type

6 Conclusions

A solar-powered, zero-bill rural house solar-driven space heating system employing an innovative multiple-throughout-flowing micro-channel solar-panels-array was

investigated from both theoretical and experimental aspects. Compared to the traditional one-to-one panels connection approach, the novel multiple-throughout-flowing mode can achieve around 10% overall solar thermal efficiency and 80% higher energy efficiency ratio (EER) while the cost of the whole panels-array remains the same between the both modes.

Compared to the one-to-one-connection mode, the multiple-throughout-flowing mode creates a higher flow speed within the panel flow channels, thus leading to a higher solar thermal efficiency for the individual panels, with the potential increase rate in the range from 7.5% to 15.4%. Furthermore, the multiple-throughout-flowing mode, by circulating the working fluid throughout the panels-array several times, can reduce the temperature difference between the head and real panels and thus increase the overall solar thermal efficiency of the array be around 10%. Last but not least, the multiple-throughout-flowing mode reduces the fluid flow turning number within the panels, thus leading to the significantly lower fluid flow resistance and thus a very higher energy efficiency rate (EER), with the potential rate in the range 62% to 68%.

The panels' number, fluid flow turning number and fluid flow speed have great impact to the performance of the multiple-throughout-flowing panels-array. It is found that the most favourite panels' number in an array is 10, associate fluid flow turning number is 5, and the fluid flow speed with the array channels is 0.3m/s.

The established analytical model in this research has a good accuracy in predicting the performance of the multiple-throughout-flow panels array, giving a discrepancy of less than 10%.

Acknowledgments:

The authors would acknowledge our appreciation to the financial supports from the DBEIS (Department for Business, Energy and Industry Strategy) – Low Carbon Heating Technology Innovation Fund 2018 for the project titled 'A Low Carbon Heating System for Existing

Public Buildings Employing a Highly Innovative Multiple-throughout-flowing Micro-channel Solar-panels-array and a Novel Mixed Indoor/outdoor Air Source Heat Pump' and from the EPSRC (EP/R004684/1) and Innovate-UK (TSB 70507-481546) for the Newton Fund – China-UK Research and Innovation Bridges Competition 2015 Project titled 'A High Efficiency, Low Cost and Building Integrate-able Solar Photovoltaic/Thermal (PV/T) System for Space Heating, Hot Water and Power Supply'.

References

[1] Xinye Zheng, Chu Wei, Ping Qin. 2014 Chinese Residential Energy Consumption Survey. CRECS, Science Press, January 2015.

[2] Bruno Lapillonne, Karine Pollier, Nehir Samci. Energy Efficiency Trends for households in the EU. Intelligent Energy Europe Programme of the European Union, May, 2015.

[3] Hadorn J-C. IEA solar and heat pump systems-Solar heating and cooling Task 44 & heat pump programme Annex 38. Energy Procedia 2012, 30:125-133.

[4] Mehmet Esen, TahsinYuksel. Experimental evaluation of using various renewable energy sources for heating a greenhouse, Energy and Buildings 2013, 65:340-351.

[5] Mehmet Esen. Thermal performance of a solar-aided latent heat store used for space heating by heat pump, Solar Energy 2000, 69(1): 15-25.

[6] D. Rojas, J. Beermann, S.A. Klein, D.T. Reindl. Thermal performance testing of flat-plate collectors. Solar energy 2008,82: 746–757.

[7] N. Molero Villar, J.M. Cejudo Lo´pez. Numerical 3-D heat flux simulations on flat plate solar collectors. Solar Energy2009, 83:1086–1092.

[8] I. Budihardjo, G.L. Morrison. Performance of water-in-glass evacuated tube solar water heaters. Solar Energy 2009, 83 (1): 49–56.

[9] Moreno-Rodríguez A, González-Gil A, Izquierdo M, Garcia-Hernando N. Theoretical model and experimental validation of a direct-expansion solar assisted heat pump for domestic hot water applications. Energy 2012, 45:704-715.

[10] E. Speyer. Solar energy collection with evacuated tubes. Energy and Power1965,

87:270–277.

[11] Diao YH, Wang S, Zhao YH, Zhu TT, Li CZ, Li FF. Experimental study of the heat transfer characteristics of a new-type flat micro-heat pipe thermal storage unit. Applied Thermal Engineering2015, 89: 871–882.

[12] Seunghyun Lee, Issam Mudawar. Investigation of flow boiling in large micro-channel heat exchangers in a refrigeration loop for space applications. International Journal of Heat and Mass Transfer 2016, 97:110–129

[13] DENG YueChao, QUAN ZhenHua, Experimental investigations on the heat transfer characteristics of micro heat pipe array applied to flat plate solar collector, SCIENCE CHINA Technological Sciences 2013, 56(5): 1177-1185.

[14] Yuechao Deng, Yaohua Zhao, Experimental investigation of performance for the novel flat plate solar collector with micro-channel heat pipe array (MHPA-FPC), Applied Thermal Engineering 2013, 54: 440 -449.

[15] Yuechao Deng, Yaohua Zhao, Experimental study of the thermal performance for the novel flat plate solar water heater with micro heat pipe array absorber, Energy Procedia 2015, 70: 41 -48.

[16] Yuechao Deng, Zhenhua Quan, Yaohua Zhao, Lincheng Wang, Zhongliang Liu. Experimental research on the performance of household-type photovoltaic–thermal system based on micro-heat-pipe array in Beijing. Energy Conversion and Management 2015, 106: 1039-1047.

[17] Yuechao Deng, Wei Wang Experimental study of the performance for a novel kind of MHPA-FPC solar water heater，Applied Energy 2013, 112: 719-726.

[18] G Li, X Zhao, J Ji. Conceptual development of a novel photovoltaic-thermoelectric system and preliminary economic analysis. Energy Conversion and Management 2016, 126, 935-943.

[19] Mert Tosun, Bahadır Doğan, M. Mete Öztürk, L. Berrin Erbay. Integration of a Mini-Channel Condenser into a Household Refrigerator with Regard to Accurate Capillary Tube Length and Refrigerant Amount. International Journal of Refrigeration 2018, https://doi.org/10.1016/j.ijrefrig.2018.11.012

[20] Seunghyun Lee, Issam Mudawar. Transient characteristics of flow boiling in large micro-channel heat exchangers. International Journal of Heat and Mass Transfer 2016, 103:186-202

[21] Jinzhi Zhou, Xudong Zhao, Xiaoli Ma, Zhenyu Du, Yi Fan, Yuanda Cheng, Xinghui Zhang. Clear-days operational performance of a hybrid experimental space heating system employing the novel mini-channel solar thermal & PV/T panels and a heat pump. Solar Energy 2017, 155: 464–477.

[22] Deli Ling, Genmao Mo, Qingtai Jiao, Jiajie Wei, Xiaojing Wang. Research on solar heating system with phase change thermal energy storage. Energy Procedia 2016, 91: 415 – 420.

[23] Federico Bava, Simon Furbo, Bengt Perers. Simulation of a solar collector array consisting of two types of solar collectors, with and without convection barrier. Energy Procedia 2015, 70: 4 – 12.

[24] Ion Visa, Macedon Moldovan, Mihai Comsit. Facades integrated solar-thermal collectors – challenges and solutions. Energy Procedia 2017, 112: 176 – 185.

[25] Zhiyong Tian, Bengt Perers, Simon Furbo, Jianhua Fan. Thermo-economic optimization of a hybrid solar district heating plant with flat plate collectors and parabolic trough collectors in series. Energy Conversion and Management 2018, 165: 92-101.

- Multiple-throughout-flow lowers temperature difference between head and rear panels
- This flow mode leads to the increased overall solar thermal efficiency by around 10%
- This flow mode leads to the increased energy efficiency factor by around 80%
- The most appropriate panel number in an array is 10
- The most appropriate fluid flow turning number is 5.